

# Assessment of potentially toxic heavy metal contamination in agricultural fields, sediment, and water from an abandoned chromite-asbestos mine waste of Roro hill, Chaibasa, India

Adarsh Kumar<sup>1</sup> · Subodh Kumar Maiti<sup>1</sup>

Received: 14 September 2014 / Accepted: 5 March 2015 / Published online: 19 March 2015  
© Springer-Verlag Berlin Heidelberg 2015

**Abstract** The major aim of the present study is to assess (1) depth-wise physico-chemical characteristics and pseudo-total metal concentrations in the abandoned chromite-asbestos mine waste, contaminated agricultural soil, and control agriculture soil; (2) degree of soil contamination and metal geoaccumulation index in agricultural soil; and (3) concentrations of metal in the sediment and water samples of river, tributary, and different water bodies located in the vicinity of an abandoned chromite-asbestos mine of Roro hill. Nutrient content and physical properties of the mine waste were found low and poor. Pseudo-total metal concentrations in the mine waste were found in the order of  $\text{Cr} > \text{Ni} > \text{Mn} > \text{Cu} > \text{Pb} > \text{Co} > \text{Zn} > \text{Cd}$ . High concentrations of Cr ( $1148 \text{ mg kg}^{-1}$ ) and Ni ( $1120 \text{ mg kg}^{-1}$ ) were found in the contaminated agricultural soils which far exceed the soil threshold limits. The contamination factor and geoaccumulation index in the agricultural soils were found high and decreased with increase in depth for Cr and Ni, indicating strong contamination. Concentrations of Zn, Mn, Co, Cu, Pb, and Cd were found low and within toxicity limit. Further, metal grouping and site grouping cluster analysis also revealed that Cr and Ni are closely linked with each other and chromite-asbestos mine waste was the major source of contamination. Sediment samples were found high in metal

content and decreased with increase in distance and mine waste influence. Water flowing from the mine adit was found high in Cr and Ni concentration (above critical drinking water total concentration). Further research is required to study the pollution factors for sediment and water samples and metal accumulation pattern in naturally growing plants and locally practised crops to access its impact on human and livestock.

**Keywords** Agriculture soil · Contamination factor · Cluster analysis · Heavy metal · Geoaccumulation index · Principle component analysis

## Introduction

The ever growing world population leading to rapid urbanization and industrialization, is extensively causing environmental problems throughout the world (Kumar and Maiti 2014; Benhaddya and Hadjel 2014). Abandonment of metal mines is one of the most important environmental concerns (Das and Maiti 2008; Mileusnic et al. 2014). There are various reasons for abandonment of mines, such as economic reasons (low commodity price or high production cost), geological surprises (low grade or size of ore body), technical (adverse geotechnical condition or equipment failure), regulatory (safety or environmental violation), social or community pressure, closure of downstream industries or markets (Maiti 2013). These abandoned and active mine waste or sites can act as continuous source of heavy metals pollution which has toxic effects on soil, water, and living biota (Fernandez-Caliani et al. 2009; Mileusnic et al. 2014). The wastes are generally very fine, loose, and homogeneous, with low bulk density and moisture-holding capacity and devoid of nutrients,

**Electronic supplementary material** The online version of this article (doi:10.1007/s12665-015-4282-1) contains supplementary material, which is available to authorized users.

✉ Adarsh Kumar  
adarsh.ese@gmail.com

<sup>1</sup> Department of Environmental Science and Engineering,  
Centre of Mining Environment, Indian School of Mines,  
Dhanbad 826004, Jharkhand, India

which not only hinders the plant colonization but also contaminates its surrounding during strong winds and heavy run-off during monsoon (Mileusnic et al. 2014; Kumar and Maiti 2014). Furthermore, the mine waste is easily carried away to agriculture fields and nearby water bodies during monsoon, and contaminates soil, sediment, water, and crops. The interaction between natural water and serpentine rocks can cause enrichment in heavy metals in water (Apollaro et al. 2011). Heavy metals easily get adsorbed and accumulated in sediments, and may exert lethal effects on the organisms when reaching significant concentrations (Tang et al. 2014).

Most of the chromite and asbestos fibers are produced by extensive opencast mining, generating enormous amount of mine waste and host rocks. The Roro hills of Chaibasa district (West Singhbhum, Jharkhand, India) have undergone extensive open cast and underground mining operations for extraction of magnetite, chromite, and asbestos and generated million tons of toxic mine waste and host rocks (Fig. 1). These wastes contain potentially toxic heavy metals, mainly chromium (Cr) along with asbestos fibers. Apart from Cr, mine wastes are generally rich in other metals which are associated with serpentine soil such as Ni and Mn (Ho et al. 2013; Kumar and Maiti 2013). Chromium and asbestos are carcinogenic and their exposure may lead to cancer, mesothelioma, pneumoconiosis, skin irritations, and other respiratory problems (Whalley et al. 1999; OSHA 2006; Bloise et al. 2008; Pugnallonia et al. 2013).

To assess the level of heavy metal pollution from mine waste, contamination factor (CF) and geoaccumulation index (Igeo) are frequently used by several researchers for predicting contamination of soil in multi-metal-contaminated agricultural field (Machender et al. 2013; Huang et al. 2013), sediments (Zhang et al. 2013; Lin et al. 2013; Wang et al. 2014), mine smelter area (Khorasanipour and Aftabi 2011), farming soils (Moghaddas et al. 2013), and pyritic soils (Fernandez-Caliani et al. 2009). Geoaccumulation index and contamination factor are single, easy to apply, and quantitative index which can be applied without considering the grain size and natural geochemical variability.

Although it is considered that bioavailable portion of toxic metals is the basis of soil risk assessment of soil contaminants, there are still only few reports which are using bioavailable metal concentration for this purpose. In most of the cases, total or pseudo-total metal concentrations are used to calculate the different soil pollution factors (Das and Maiti 2008; Kumar and Maiti 2014).

The major aim of the present study is to assess (1) depth-wise physico-chemical characteristics and pseudo-total metal concentrations of abandoned chromite-asbestos mine waste (CMW), contaminated agricultural soil 1 and 2 (CAS1 and CAS2), and control agriculture soil (CS); (2) degree of soil contamination and metal enrichment in agricultural soil; and (3) concentrations of metal in the sediment and water samples of river, tributary, and



**Fig. 1** Distant view of the abandoned chromite-asbestos mine waste of the Roro hills located in Chaibasa district of West Singhbhum, Jharkhand, India. Number 1 and 4 are the boulders and small rock mine waste produced during the extraction of chromite and asbestos from the parent material. Number 2 and 3 are the fine sand-textured chromite-asbestos mine waste which was crushed down to obtain asbestos fibers along with chromium. The entire mine waste together

acts as continuous source of pollution to the surroundings due to wind and water erosion. Tributaries flowing from the hill also cause gully erosion (clearly seen in number 2 and 3). Other parts of the hill, where toxic waste was not found layed down, dense growth of trees was noticed. All the mine waste is located next to the adits from which it is being excavated

different water bodies located in the vicinity of abandoned chromite-asbestos mine of Roro hill.

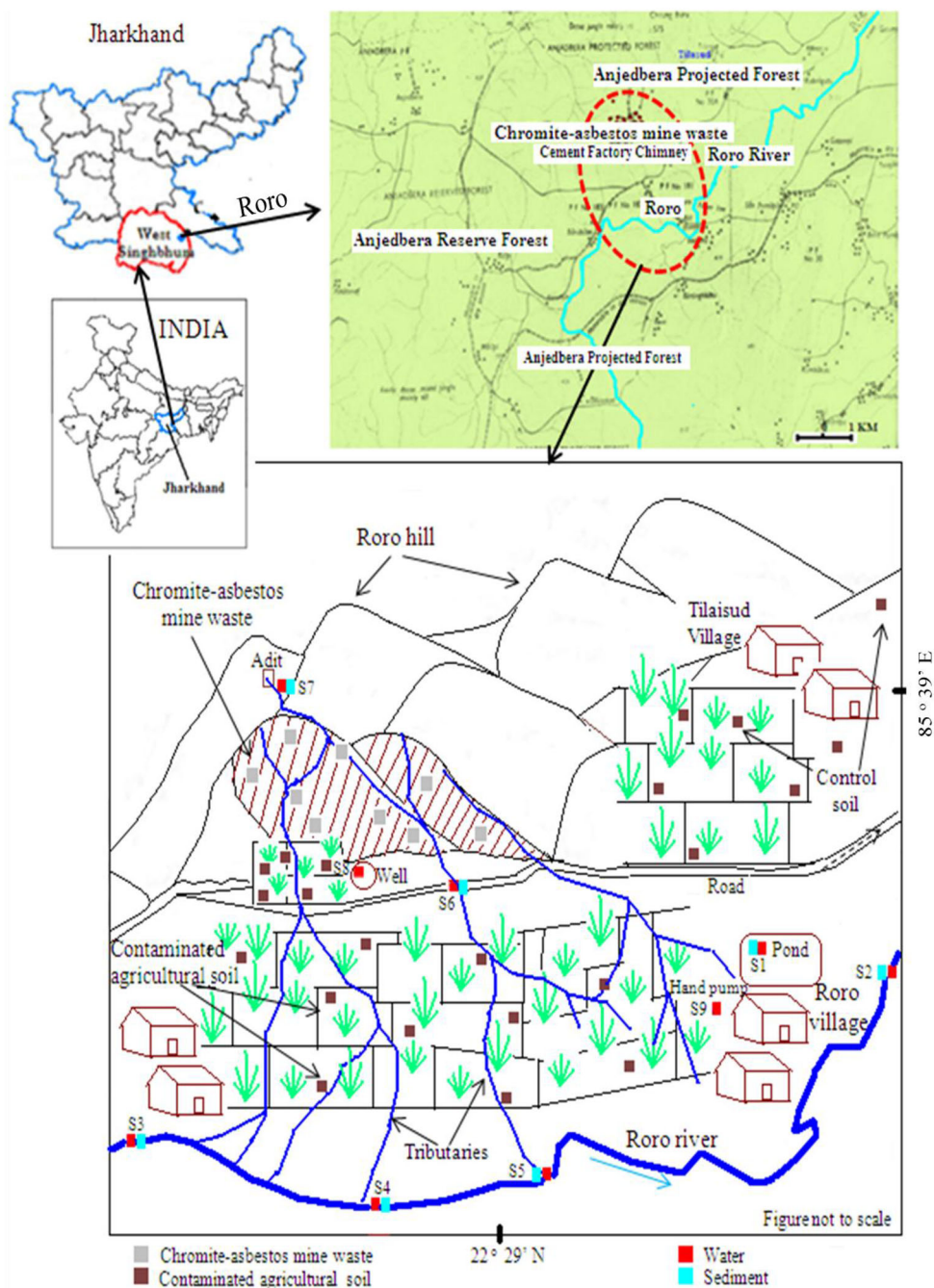
## Materials and methods

### Study area, geology, and mineralization

Abandoned chromite-asbestos mine of Roro hill ( $N22^{\circ}29'$ ,  $E85^{\circ}39'$ ) is located 22 km away from Chaibasa district of Jharkhand, India (Fig. 2). Nearly, 0.7 million tons of toxic

asbestos waste mixed with chromite-bearing host rock were being left since 1983. No major scientific study so far has been carried out to assess the fate and impact of the abandoned mine waste materials on the agricultural soil, crops, naturally growing plant species, water, and sediment. Abandoned mine wastes are spread over approximately 100 m at the top and 400 m down-slope of the hill, and further extends to the agriculture fields situated at the foothills. About 40 cm of thick CMW deposited over the agriculture fields is imparting deleterious effect on the environmental and human health. The perennial water

**Fig. 2** Location map and sampling sites of the Roro hills, West Singhbhum, Jharkhand, India



flowing from the hill relocates large volume of toxic mine waste by intensive rainfall and wind erosion and meets the Roro river carrying high concentration of toxic metals.

In the Roro area, the chromite-bearing ultramafic rocks of Archaean age are emplaced within the meta-sedimentary rocks of the Iron Ore Super Group represented in the area by shale, phyllite, slate, quartzite, chert, dolomitic limestone, and altered basic lava of the Singhbhum Craton (Fig. 3). Laterization of the ultramafic rocks was found to be one of the common features of this region. In the Roro-Jojohatu areas, the ultramafic rocks along with the country rocks were co-folded into a major easterly closing synformal structure in a single deformation stage. A band of high-grade chromite ore with a thickness of 0.3 m could be traced in the Roroburu persistently more than 1.6 km along the contact of pyroxenite and peridotite. The ultramafic rocks are metamorphosed into greenschist to amphibolite facies. Chromite ore bodies are confined mainly to the dunites and pyroxenites and are concentrated to the margin of the ultrabasic rocks. The growth of ferrochromite to magnetite along its border or along fracture of the chromite grains was observed in the Roro chromites. The massive chromites show a narrow range of  $\text{Cr}_2\text{O}_3 = 56.42\text{--}59.06$  wt%,  $\text{Al}_2\text{O}_3 = 9.16\text{--}9.86$  wt%,  $\text{MgO} = 10.26\text{--}10.94$  wt%, and  $\text{TiO}_2 = 0.29\text{--}0.47$  wt% (GSI 2010).

The climate of study area is tropical, characterized by high annual precipitation of approximately 1422 mm within 4 months (July–October) with peak summer (April–June) of extreme high temperature (46 °C) and cold winter (November–March). Currently, the region of the chromite-asbestos mine is considered to be a hot spot of pollution for the entire region. Wind blow, water run-off, and illegal use of this fine toxic waste as filling material for construction of roads pits are continuously creating environmental

concern for the local populations. Children of the local villagers inhale and come in contact with this waste while playing on the hill resulting in skin rashes, nose bleeding, inhalation of asbestos fibers, and other health issues (Fig. 4a–d).

### Soil sampling and analyses

The soil samples for three different profiles of 0–15 cm (rhizospheric soil), 15–30 cm, and 30–45 cm depth were collected using core from four different locations (1) chromite-asbestos mine waste (CMW,  $n = 9$ ); (2) contaminated agricultural soils (CAS1) (located on the foot hill,  $n = 5$ ); (3) contaminated agricultural soils (CAS2) (located 500 m away from the mine waste,  $n = 5$ ); and (4) control soil (CS) (referred as reference site, located at 1000 m away, free from contamination;  $n = 5$ ). CMW samples were collected randomly from abandoned mine waste dump by considering the whole dump as a single sampling unit. Each sample was a composite of four bulked sub-samples and was prepared using Coning and quartering method. By removing the top vegetation cover and litter fall, all the samples were collected and filled in polypropylene zip bags and brought to the laboratory. The samples were air dried for 3 days, oven dried at 105 °C, allowed to pass through stainless steel nylon sieve below <1 mm, and kept in polypropylene air tight zip bags for further analysis.

The general physico-chemical characteristics of chromite-asbestos mine waste, agricultural soils, and control soils were determined using standard methods. Particle size distribution (PSD) was determined by sieving method (Gee and Bauder 1986). Water holding capacity (WHC) was determined using Keen's box, whereas bulk density

**Fig. 3** Detailed geological map of the area around Roro-Jojohatu area, Singhbhum, India (GSI 2010)

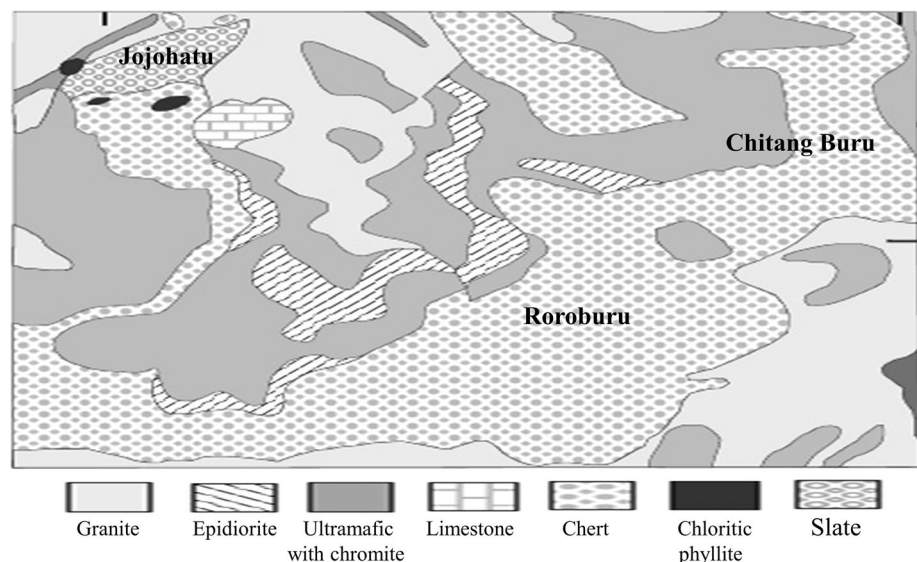




**Fig. 4** Pictorial diagrams showing **a** local children playing on the slope of chromite-asbestos mine waste (CMW); **b** naturally growing plant on the top of the abandoned CMW hill; **c** widespread of CMW

on hill slope, agricultural fields, natural vegetative area, and fallow lands; **d** illegal loading and use of toxic mine waste as filling material in the construction of the roads etc

(BD) by metal core sampler method (Mukhopadhyay et al. 2013). Pore space (PS, porosity) was determined from BD measurements with an assumed particle density of  $2.65 \text{ Mg m}^{-3}$  (Sobek et al. 1978). The pH and electrical conductivity (EC) of the soil samples were measured in a soil–water suspension (1:1; soil:deionised water) using pH meter (Cyberscan 510) and conductivity meter (EI 601), respectively (Maiti 2013). Organic carbon (OC) was determined by rapid dichromate oxidation method (Walkley and Black 1934). Available phosphorus (Av. P) was determined by Olsen method (Olsen and Sommers 1982) using UV–Visible Spectrophotometer (UV 265, Shimadzu) and available nitrogen (Av. N) by alkaline permanganate method (Subbiah and Asija 1956). Cation exchange capacity (CEC) was determined using 1 N ammonium acetate extraction method (Jackson 1973) using Flame photometer (Systronics 128) (Das and Maiti 2008; Li et al. 2011). Total metal concentrations were determined by digesting accurately weighed 1 g of waste or soil samples using  $\text{HNO}_3$  conc. (69–71 %, Rankem), HF (40 %, Rankem),  $\text{HClO}_4$  (71–73 %, Rankem) (5:1:1; v/v/v) in Teflon vessels till the complete dissolution of the sample was achieved (Zhao et al. 2009; Ho et al. 2013). Pseudo-total (conc.  $\text{HNO}_3$  (1:1 w/v slurry); 30 %  $\text{H}_2\text{O}_2$  and HCl) metals were determined using USEPA 3050B method. Digested samples were warmed with 1 %  $\text{HNO}_3$ , filtered (Whatman #42 filter, pore size  $2.5 \mu\text{m}$ ), made up the volume up to 100 mL with the same using standard volumetric flask, and

stored in polyethylene bottles at  $4^\circ\text{C}$ . Metal concentrations of all the samples were analyzed using a flame atomic absorption spectrophotometer (FAAS-GBC Avanta, Australia) at the most sensitive resonance wave length, respective to each element.

### Sediment and water sampling and analyses

A total of seven sediments and nine water samples were collected from different locations which include river, pond, well, and tributary flowing from the adits (Table 1). The grab sediment samples were air dried for 3 days, oven dried at  $105^\circ\text{C}$ , allowed to pass through nylon sieve below  $<1 \text{ mm}$  and kept in polypropylene air tight zip bags for further analysis. Accurately weighed 0.2 g of sieved sample was taken in Teflon crucible and digested with mixture of conc. HF acid, 1:1  $\text{H}_2\text{SO}_4$  acid, and 0.5 N HCl acid (8 mL + 5 mL + 5 mL) on hot plate for analysis of metals (Co, Cr, Cu, Mn, Ni, and Zn). For analysis of Pb, similarly 0.2 g of sieved sample was digested with mixture of HF acid and 3 %  $\text{HNO}_3$  acid (3 mL + 5 mL) on hot plate (APHA 2012). The digested samples were then filtered through Whatman filter paper no. 42 and volume was made 100 mL with double distilled water and analyzed in FAAS.

The grab water samples were collected in 2-L capacity polypropylene jerry cans, previously soaked and washed with 10 %  $\text{HNO}_3$  and double distilled water and sealed

**Table 1** Description and sampling location of the sediment and water samples collected from Roro hill and its vicinity

Sample no.	Description and sampling location
S1	Pond (200 m from the hill)
S2	Roro river (4000 m from the hill)
S3	Roro river (Upstream, 1000 m from the hill)
S4	Roro river (Downstream, 700 m from the hill)
S5	Tributary (water mixing with Roro river, 2300 m from hill)
S6	Adit water (flowing from the underground mining site from the top of the hill)
S7	Tributary flowing from the hill (on the mid of the hill)
S8*	Well water (on the foot of the hill)
S9*	Hand-pump water (400 m from hill)

\* Only water samples were collected

properly to prevent overflow. Preservation of water samples were done in the laboratory by lowering the pH < 2 using HNO<sub>3</sub> (Analytical reagent grade) and kept at 4 °C in refrigerator. For the analysis of heavy metals, 1-L of water sample was concentrated to 50 mL by volume in a Kjeldahl flask by using 5 mL of conc. HNO<sub>3</sub> (to eliminate the organic matter interference). The concentrated solution was filtered through Whatman No. 42 filter paper and used for metal analysis (Co, Cr, Cu, Mn, Ni, Pb, and Zn) by FAAS.

### Soil pollution indices

To assess the impact of pollution, different soil pollution indices (contamination factor and geoaccumulation index) are calculated as follows:

**Contamination factor (CF)** It is the assessment of metal contamination in respect to control soil and calculated as (Hakanson 1980; Silva et al. 2014; Cicchella et al. 2014):

$$\text{Contamination factor (CF)} = \frac{[C]_{(\text{heavymetal})}}{[C]_{(\text{background})}} \quad (1)$$

where  $[C]_{(\text{heavymetal})}$  is the concentration of each metal in contaminated soil, and  $[C]_{(\text{background})}$  is the concentration of each metal in non-contaminated or unpolluted control soil. The contamination levels may be classified based on their intensities on a scale ranging from 1 to 6 as follows:

CF = 0: none; CF = 1: none to medium; CF = 2: moderate; CF = 3: moderate to strong; CF = 4: strongly polluted; CF = 5: strong to very strong; and CF = 6: very strong. The highest number indicates that the metal concentration is 100 times greater than what it could be expected in the crust.

**Geoaccumulation index (I<sub>geo</sub>)** It is the assessment of contamination by comparing the current and past concentrations originally used with bottom soil or sediment and was

determined using Muller's (Muller 1969; Khorasanipour and Aftabi 2011; Machender et al. 2013) expression:

$$\text{Geoaccumulation index (I}_{\text{geo}}) = \log_2 \left[ \frac{(\text{Metal})_s}{1.5(\text{Metal})_b} \right], \quad (2)$$

where  $(\text{Metal})_s$  is the concentration of metals examined in soil samples, and  $(\text{Metal})_b$  is the geochemical background concentration of the metal. Factor 1.5 is the background matrix correction factor due to lithospheric effects. The geoaccumulation index consists of seven grades or classes as follows:

$I_{\text{geo}} \leq 0$ : practically uncontaminated;  $0 < I_{\text{geo}} < 1$ : uncontaminated to moderately contaminated;  $1 < I_{\text{geo}} < 2$ : moderately contaminated;  $2 < I_{\text{geo}} < 3$ : moderately to heavily contaminated;  $3 < I_{\text{geo}} < 4$ : heavily contaminated;  $4 < I_{\text{geo}} < 5$ : heavily to extremely contaminated; and  $5 < I_{\text{geo}}$ : extremely contaminated and can be hundredfold greater than the geochemical background value.

### Quality assurance and quality control

For quality assurance and quality control (QA/QC), proper handling and care were taken during the whole process from sample collection at the field to analyses in the laboratory to avoid sample contamination and to obtain reliable data. All analytical grade or supra-pure quality reagents were used. All glassware used were soaked in nitric acid and cleaned properly. Reagent blanks, duplicates, and spiked samples were used. All the samples were prepared using double deionised Millipore water (Milli-Q system, Millipore). Standard Reference Materials (AccuTrace, AccuStandard Inc., USA; Matrix 2–5 % nitric acid; CRM uncertainty  $\pm 5$  %; verified against NIST SRM# 3108 for Cd; 3112a for Cr; 3136 for Ni; 3128 for Pb; 3132 for Mn; 3168a for Zn; 3113 for Co; and 3114 for Cu) were used for the preparation and calibration of each analytical batch. Calibration coefficients were maintained at a high level  $\geq 0.99$ . Precision and accuracy of the analysis were checked by means of duplicate analysis of the selected samples (less than 10 % relative variation). Inter batch variations were monitored by repeated analysis of selected samples in various analytical batches (less than 10 % relative variation). The accuracy of the analytical procedure adopted for FAAS analysis was checked by running standard solutions after every 15 samples.

### Statistical analyses

The statistical analyses were conducted to determine mean, minimum, maximum, and standard deviation by using Data Analysis package of MS Excel 2007 (Microsoft Inc.).

Analysis of variance (ANOVA) and Multivariate analysis of variance (MANOVA) were carried out to compare the means of different combinations and parameters. Where significant F value was observed, differences between individual means were tested using DMRT (Duncan's Multiple Range Test) at 5 % level of significance. Hierarchical cluster analysis (CA) was performed on the normalized dataset of heavy metals and to group the similar sampling sites with depth by using Ward's method with Euclidean distances as measure of similarity (Varol et al. 2013). Principal component analysis (PCA) was performed for the metal concentration in soil (Moghaddas et al. 2013; Mathivanan and Rajaram 2014). Normalized variables (original variables) were transformed into the rotated components to extract the significant principal components (reducing the contribution of variables with minor significance). Further, these principal components were subjected to Varimax rotation and Kaiser-Meyer-Olken (KMO) test (eigen value > 1 and loading coefficient > 0.10) to generate PC factors/groups and to find out suitability of data for PCA. All the data were executed using SPSS 16.0 (SPSS Inc. Chicago, USA) and XLSTAT 2007 package.

## Results and discussion

### Physico-chemical characteristics of soils

The PSD and other different physical and chemical characteristics of CMW, CAS1, CAS2, and CS under varying depth of 0–15 cm, 15–30 cm, and 30–45 cm are presented in Figs. 5 and 6. PSD varied substantially from site to site which reveals that mining activities have caused disturbances in this area. CMW, CAS1, and CAS2 are mainly composed of sand with a maximum mean value of 95.6 % in the top layer of CMW and minimum mean value of 90.5 % in the CAS2. Ho et al. (2013) had also reported higher percentage of sand content in the serpentine soil of Wan-Ron Hill of Tiwan. The maximum silt and clay content of 24 % was found for control soil. It was found that the percentage of sand decreases with increase in the depth for all the soils and mine waste. BD was also found high in CMW, CAS1, and CAS2 soil as compared to CS. Because of the high sandy texture and BD, WHC and PS for CMW and CASs for all the profiles were found low and ranged between 22–30 % and 38–44 %, respectively, whereas in case of CS it ranged between 32–34 % and 48–51 %, respectively.

The pH value for all the soil samples ranged between neutral to slightly alkaline. The EC, OC, Av. N, and Av. P were found very low in the CMW and CAS2. Low nutrient availability in the agricultural fields was found because of

the spreading and deposition of mine waste from the hill into the surrounding area which was occurring mainly during monsoon and summer season, whereas these values were found slightly higher in case of CAS1 may be because of the addition of organic manures or P-fertilizer (Phosphorous-fertilizer) in the agricultural field by the local farmers. Das et al. (2013) also reported lower availability of nutrients mainly N, P, K, and OC in the chromite overburden dump. A significant increase was found in the EC, OC, Av. N, and Av. P in third profile (30–45 cm) of CAS2. The possible reason for the sufficient nutrient availability in this profile could be because of the farther allocation resulting in thin-layer deposition of mine waste in the lower depth and non-influence of this agricultural soil from CMW. The CEC ranged between 0.47 and 0.56  $\text{cmol}(+) \text{kg}^{-1}$  for the mine waste in all the three profiles. In case of CAS2, minimum CEC was found in the top profile (3.48  $\text{cmol}(+) \text{kg}^{-1}$ ), whereas maximum in the bottom profile (4.8  $\text{cmol}(+) \text{kg}^{-1}$ ). Exchangeable cations (Exc. K, Ca, and Na) were found very low in the CMW and CASs because of the higher influence of CMW in this area.

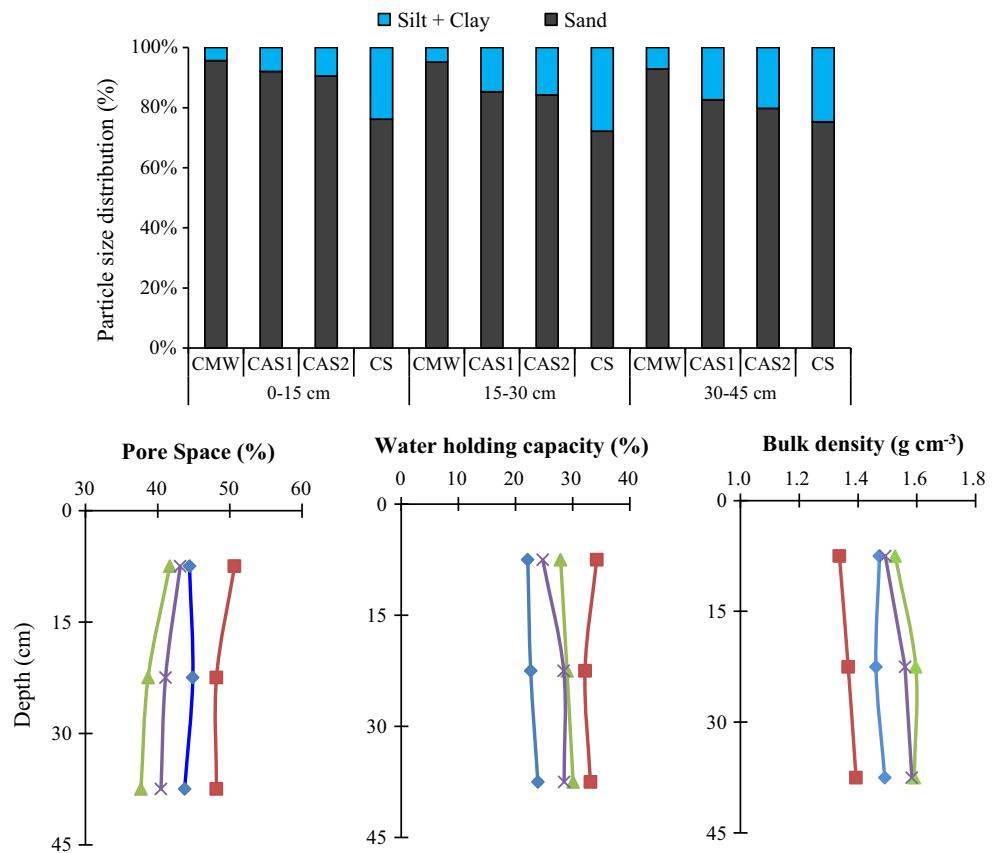
### Pseudo-total metal content and soil pollution indices of soils

The pseudo-total metal content of eight heavy metals in CMW, CAS1, CAS2, and CS in the three different profiles of 0–15 cm, 15–30 cm, and 30–45 cm are statistically ( $p < 0.05$ ) presented in Table 2. High metal concentrations were found in the order of  $\text{Cr} > \text{Ni} > \text{Mn} > \text{Cu} > \text{Zn} > \text{Co} > \text{Pb} > \text{Cd}$ . Significant differences ( $p < 0.05$ ) were found between the metal content of different sampling sites for the same profile. However, for most of the metals, no significant differences were found in CMW, CAS1, and CAS2, suggesting possibility of CMW as a source of metal contamination for the agricultural soils. The average pseudo-total metal concentrations in all profile (0–45 cm) of CMW, CAS1, and CAS2 ranged between 215–2125  $\text{mg Cr kg}^{-1}$ ; 108–1280  $\text{mg Ni kg}^{-1}$ ; 18–47  $\text{mg Zn kg}^{-1}$ ; 212–444  $\text{mg Mn kg}^{-1}$ ; 4–11  $\text{mg Co kg}^{-1}$ ; 12–36  $\text{mg Cu kg}^{-1}$ ; 2–10  $\text{mg Pb kg}^{-1}$ ; and 0.1–1.1  $\text{mg Cd kg}^{-1}$ . The CF and Igeo for the metals were generally found in the order of  $\text{Ni} > \text{Cr} > \text{Cd} > \text{Cu} > \text{Co} > \text{Mn}$  and  $\text{Zn}$  (Table 3). The critical ranges of heavy metals in soil and guidelines for safe limits of some metals in agricultural soil ( $\text{mg kg}^{-1}$ ) are presented in Table 4.

#### Chromium (Cr) and nickel (Ni)

Chromium exists in nature in  $\text{Cr}^{3+}$  and  $\text{Cr}^{6+}$  form. The average Cr concentration of 100  $\text{mg kg}^{-1}$  exists in the earth's crust (Alloway 2013). The trend and variations of Cr differ considerably with different soil type and profiles.

**Fig. 5** Physical properties of chromite-asbestos mine waste, contaminated agriculture soils, and control soil in the three different depth profiles of 0–15 cm, 15–30 cm, and 30–45 cm. Shapes representing the samples: *diamond*—CMW; *triangle*—CAS1; *cross*—CAS2 and *square*—CS

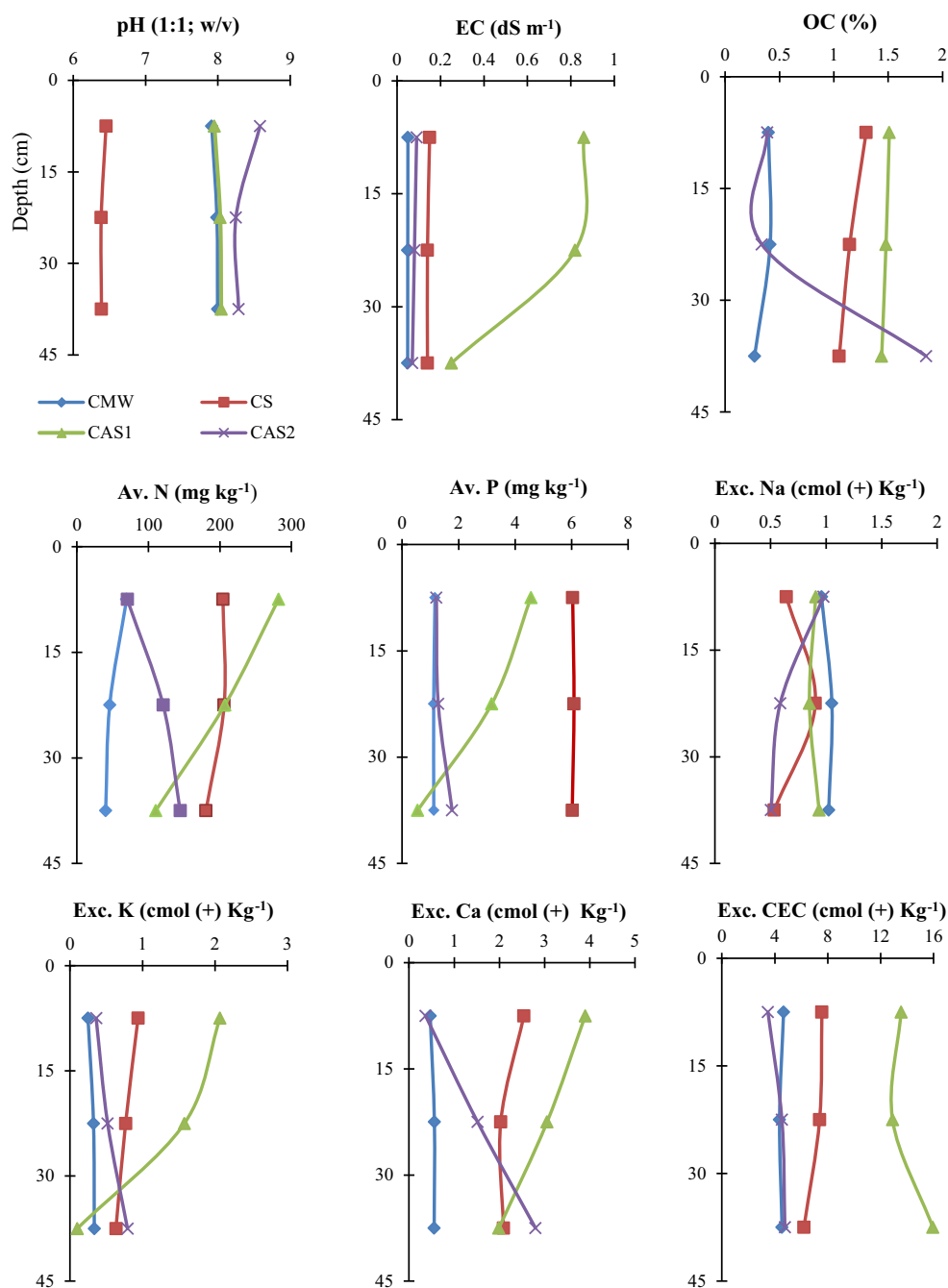


Concentration of Cr in all the CMW and CAS1 and CAS2 samples was found very high and above the critical soil total concentration of  $75\text{--}100\text{ mg kg}^{-1}$  (Alloway 2013). Significant differences ( $p < 0.05$ ) were found for the pseudo-total metal content in different sampling sites for the same profile. High concentration of Cr ranged between  $1345\text{--}2702\text{ mg kg}^{-1}$ ,  $1101\text{--}1195\text{ mg kg}^{-1}$  and  $1098\text{--}1120\text{ mg kg}^{-1}$  was found in the top profile of CAW, CAS1, and CAS2, respectively. The percentage values of pseudo-total Cr concentration of 88, 58, and 62 % of total content (data not shown) were found in the top profile of CAW, CAS1, and CAS2, respectively. Such type of high concentrations of Cr normally shows serpentine nature of the soil with average Cr concentration of  $3000\text{ mg kg}^{-1}$  (Alloway 2013). Reeves et al. (2007) had also reported high Cr concentration of  $1400\text{--}3640\text{ mg kg}^{-1}$  in the serpentine soils of Santa Elena peninsula, Costa Rica. The total Cr concentration varied from  $0.5\text{--}250\text{ mg kg}^{-1}$  with an average range of  $40\text{--}70\text{ mg kg}^{-1}$  in normal soil (Alloway 2013). High concentration of Cr in the mine waste could be because of the mining of hills to extract chromite ores from mafic and ultramafic rocks, which typically remains associated with the  $\text{MgO}$ ,  $\text{Al}_2\text{O}_3$ , and  $\text{SiO}_2$ . The highest mean pseudo-total Cr concentration was found in the top layer of CMW ( $2124\text{ mg kg}^{-1}$ ) and decreased with

increase in depth and distance in soil samples. All the layer of CAS1 and CAS2 are highly contaminated with Cr because of the thick deposition of CMW which is rolling down from the hill, get transported through water and wind and deposited into the agricultural fields during summer, winter, and monsoon. However, lower concentration of Cr was found in the bottom layer of CAS2 as compared to other two layers because of its farther distance, resulting in thin deposition of CMW in this agricultural field. Addition of P-fertilizer could be one of another possible reason for the increase of Cr concentration in CAS1 as compared to CAS2 (Huang et al. 2013; Wang et al. 2014). The CF for CMW, CAS1, and CAS2 were found above 6, which represents that the soil is very strongly contaminated with Cr. The CF values had increased with increase in depth and maximum CF was found for CMW (18.07) of 30–45 cm depth soil, whereas minimum for CAS2 (1.98). Similarly, Igeo was ranged between 0.4 and 3.6 which represents that all the soils are moderately to heavily contaminated with Cr.

Ni is mostly associated with the Cr and presents in all rock types from traces to relatively high concentration. High concentrations of Ni are particularly found in serpentine soil ( $2000\text{ mg kg}^{-1}$ ) and normally  $80\text{ mg kg}^{-1}$  exist in the earth's crust (Adriano 2001). Significant differences ( $p < 0.05$ ) were found for the metal content in

**Fig. 6** Chemical characteristics of chromite-asbestos mine waste, contaminated agriculture soil, and control soil in the three different profiles of 0–15 cm, 15–30 cm, and 30–45 cm. Shapes representing the samples: *diamond*—CMW; *triangle*—CAS1; *cross*—CAS2 and *square*—CS. *EC* electrical conductivity, *OC* organic carbon, *CEC* cation exchange capacity, *Al*, available, *Exc.* exchangeable



different sampling sites for the same profile. The Ni concentration in the CMW and CASs was found very high and above the critical soil total concentration (100 mg kg<sup>-1</sup>). High concentration of Ni in the top profile of CMW, CAS1, and CAS2 was found ranged between 945–1620 mg kg<sup>-1</sup>, 1099–1160 mg kg<sup>-1</sup>, and 1115–1280 mg kg<sup>-1</sup>, respectively. Das et al. (2013) had reported Ni concentration of 224–523 mg kg<sup>-1</sup> in the chromite dump of Sukinda, India. High concentration of 691–1220 mg kg<sup>-1</sup> of Ni was reported in the abandoned site of serpentine mine, Wan-Ron hill, Taiwan (Ho et al. 2013). Percentage values of pseudo-

total Ni concentration were about 96, 95, 92, and 71 % in the top profile of CMW, CAS1, CAS2, and CS of its total metal content (data not shown), respectively. These high Ni concentrations represent normally found average Ni concentration (2000 mg kg<sup>-1</sup>) in the serpentine soil (Alloway 2013). However, the total Ni concentration varied from 0.2 to 450 mg kg<sup>-1</sup> with a world average of 22 mg kg<sup>-1</sup> in normal soil (Alloway 2013). Total Ni concentration of 101 mg kg<sup>-1</sup> was found in the top layer of CS. Because of the association of Ni with Cr in serpentine soils and close ionic radii of Ni (II)<sup>+</sup> with Mg(II)<sup>+</sup> and Fe(III)<sup>+</sup>, ionic

**Table 2** Pseudo-total metal concentrations ( $\text{mg kg}^{-1}$ ) in the three different profiles of CMW, CAS1, CAS2, and CS

Depth (cm)	Sampling site	Cr	Ni	Zn	Mn	Co	Cu	Pb	Cd
0–15	CMW	2124.56 $\pm$ 519.29a (1345–2702)	1225.11 $\pm$ 218.35a (945–1620)	31.78 $\pm$ 6.16c (23–42)	443.83 $\pm$ 74.96a (325.5–568)	10.4 $\pm$ 4.47a (4.5–20.2)	35.54 $\pm$ 8.78a (21.5–45.5)	8.27 $\pm$ 2.1b (5.5–11.5)	1.11 $\pm$ 0.17a (0.85–1.31)
	CAS1	1147.67 $\pm$ 47b (1101–1195)	1120.33 $\pm$ 34.39a (1099–1160)	47.33 $\pm$ 12.71b (39.5–62)	391.33 $\pm$ 64.5a (345–465)	8.25 $\pm$ 0.79ab (7.77–9.1)	23.88 $\pm$ 4.73b (18.55–27.55)	8.1 $\pm$ 0.5b (7.6–8.6)	0.78 $\pm$ 0.03b (0.75–0.81)
	CAS2	1112.33 $\pm$ 12.42b (1098–1120)	1195 $\pm$ 82.61a (1115–1280)	43.49 $\pm$ 4.01bc (39.58–47.6)	371.33 $\pm$ 26.5a (345–398)	7.24 $\pm$ 0.37ab (6.88–7.62)	24.2 $\pm$ 2.32b (22.55–26.85)	7.03 $\pm$ 0.31b (6.70–7.30)	0.51 $\pm$ 0.09c (0.45–0.61)
	CS	168 $\pm$ 13.89c (152–177)	45.33 $\pm$ 7.02b (38–52)	101.2 $\pm$ 12.4a (92.8–115.5)	227.33 $\pm$ 11.24b (215–237)	4.04 $\pm$ 0.17b (3.88–4.21)	11.4 $\pm$ 0.85c (10.5–12.2)	30.5 $\pm$ 7.81a (21.5–35.5)	0.25 $\pm$ 0.03d (0.22–0.27)
15–30	CMW	1964 $\pm$ 233.98a (1620–2250)	1278 $\pm$ 93.07a (1145–1445)	29.94 $\pm$ 3.02c (25.5–36)	421 $\pm$ 95.97a (289–589)	11.11 $\pm$ 1.89a (8.2–13.5)	30.89 $\pm$ 4.23a (24.5–38.5)	5.77 $\pm$ 1.77c (3.58–9.24)	0.81 $\pm$ 0.08a (0.68–0.89)
	CAS1	1018.33 $\pm$ 92.51b (925–1110)	1089.67 $\pm$ 100.33b (985–1185)	41.75 $\pm$ 6.14b (36.5–48.5)	400 $\pm$ 11.53a (389–412)	9.5 $\pm$ 0.53a (8.9–9.9)	25.75 $\pm$ 3.9a (23.5–30.25)	9.79 $\pm$ 0.51b (9.25–10.25)	0.67 $\pm$ 0.08b (0.6–0.75)
	CAS2	772.33 $\pm$ 78.59b (688–825)	317 $\pm$ 8c (309–325)	21.22 $\pm$ 0.86d (20.25–21.96)	307 $\pm$ 12.12ab (300–321)	4.24 $\pm$ 0.46b (3.77–4.69)	13.27 $\pm$ 0.78b (12.5–14.05)	2.7 $\pm$ 0.05d (2.65–2.75)	0.5 $\pm$ 0.05c (0.45–0.55)
	CS	118 $\pm$ 6.55c (112–125)	41.33 $\pm$ 6.44d (35.5–48.25)	87.85 $\pm$ 6.92a (80.25–93.8)	208.66 $\pm$ 17.89b (189–224)	2.87 $\pm$ 0.12b (2.74–2.99)	30.51 $\pm$ 1.71a (29.5–32.5)	21.67 $\pm$ 1.24a (20.25–22.55)	0.25 $\pm$ 0.02d (0.22–0.27)
30–45	CMW	1961.89 $\pm$ 242.81a (1555–2220)	1280.44 $\pm$ 119.16a (1045–1399)	27.63 $\pm$ 4.15b (20.25–32.5)	373.22 $\pm$ 20.12a (339–401)	7.43 $\pm$ 1.47a (4.5–9.1)	30.31 $\pm$ 3.92a (25.5–36.7)	9.19 $\pm$ 1.53b (6.58–11.5)	0.7 $\pm$ 0.08a (0.65–0.85)
	CAS1	928 $\pm$ 53.51b (875–982)	1122.33 $\pm$ 23.01b (1099–1145)	30.42 $\pm$ 2.01b (28.5–32.5)	302.67 $\pm$ 8.02b (295–311)	6.3 $\pm$ 0.78a (5.55–7.1)	23.17 $\pm$ 4.04b (19.5–27.5)	4.96 $\pm$ 0.72c (4.25–5.68)	0.63 $\pm$ 0.02b (0.61–0.65)
	CAS2	214.5 $\pm$ 29.58c (181–237)	107.73 $\pm$ 10.46c (96.5–117.2)	17.75 $\pm$ 3.63c (14.25–21.5)	211.53 $\pm$ 6.6c (204.5–217.6)	3.93 $\pm$ 0.08b (3.88–4.02)	12.04 $\pm$ 3.13c (9.56–15.55)	2.04 $\pm$ 0.04d (2.01–2.09)	0.12 $\pm$ 0.01c (0.11–0.13)
	CS	108.6 $\pm$ 7.88c (102.5–117.7)	46.2 $\pm$ 1.54c (44.5–47.5)	91.7 $\pm$ 5.65a (85.5–96.8)	185.53 $\pm$ 14.98c (172.5–201.9)	1.66 $\pm$ 0.03c (1.62–1.68)	7.7 $\pm$ 0.62c (6.99–8.12)	20.43 $\pm$ 1.04a (19.5–21.55)	0.17 $\pm$ 0.03c (0.14–0.19)

Different alphabetical letters in the same column for the same depth represent significant difference at  $p < 0.05$  according to Duncan's multiple range test. Mean  $\pm$  standard deviation. Values in the parenthesis are the minimum and maximum range value

CMW chromite-asbestos mine waste, CAS1 contaminated agricultural soil located on the foot hill, CAS2 contaminated agricultural soil located away from the hill, CS control soil

**Table 3** Contamination factor (CF) and geoaccumulation index (I<sub>geo</sub>) of CMW, CAS1, and CAS2

Depth (cm)	Sampling site	Cr	Ni	Zn	Mn	Co	Cu	Pb	Cd
Contamination factor (CF)									
0–15	CMW	12.65	27.02	0.31	1.95	2.58	3.12	0.27	4.50
	CAS1	6.83	24.71	0.47	1.72	2.04	2.10	0.27	3.16
	CAS2	6.62	26.36	0.43	1.63	1.79	2.12	0.18	2.08
15–30	CMW	16.64	30.92	0.34	2.02	3.87	1.01	0.27	3.24
	CAS1	8.63	26.36	0.48	1.92	3.31	0.84	0.45	2.68
	CAS2	6.55	7.67	0.24	1.47	1.48	0.43	0.12	2.00
30–45	CMW	18.07	27.72	0.30	2.01	4.49	3.94	0.45	4.49
	CAS1	8.55	24.29	0.33	1.63	3.80	3.01	0.24	3.76
	CAS2	1.98	2.33	0.19	1.14	2.37	1.56	0.10	0.72
Geoaccumulation index (I <sub>geo</sub> )									
0–15	CMW	3.08	4.17	−2.26	0.38	0.78	1.06	−2.47	1.58
	CAS1	2.19	4.04	−1.68	0.20	0.45	0.48	−2.50	1.08
	CAS2	2.14	4.14	−1.80	0.12	0.26	0.50	−3.04	0.47
15–30	CMW	3.47	4.37	−2.14	0.43	1.37	−0.57	−2.50	1.11
	CAS1	2.52	4.14	−1.66	0.35	1.14	−0.83	−1.73	0.84
	CAS2	2.13	2.35	−2.63	−0.03	−0.02	−1.79	−3.59	0.42
30–45	CMW	3.59	4.21	−2.31	0.42	1.58	1.39	−1.74	1.58
	CAS1	2.51	4.02	−2.17	0.12	1.34	1.00	−2.63	1.33
	CAS2	0.40	0.64	−2.95	−0.40	0.66	0.06	−3.91	−1.06

**Table 4** Critical range of heavy metals in soil, guidelines for safe limits of metals in agricultural soil, water and results of present study

	Cr	Ni	Mn	Zn	Co	Cu	Pb	Cd
Critical soil total concentration (Alloway 1990, 2013)	75–100	100	1500–3000	70–400	25–50	60–125	100–400	3–8
Chromite-asbestos mine waste (CMW)*	1450–3120	985–1658	412–675	39–84	45–89	102–154	68–105	1.0–1.6
Control soil (unpolluted, CS)*	152–177	38–52	215–237	92–115	3.8–4.2	11–12	22–36	0.2–0.3
Safe limits in agricultural soil								
Indian standard (Awasthi 2000)	–	75–150	–	300–600	–	135–270	250–500	3–6
European community commission ECC (Mushtaq and Khan 2010)	100	30–45	–	150–300	–	50–140	50–300	1–3
Contaminated agricultural soil 1 (CAS1)*	1885–2140	1120–1225	415–501	68–83	53–65	66–73	80–91	1.2–1.4
Contaminated agricultural soil 2 (CAS2)*	1645–1850	1245–1355	465–523	68–76	50–61	63–76	46–61	1.1–1.2
Critical drinking water total concentration (mg L <sup>−1</sup> ) (IS 10500 2012)	0.05	0.02	0.10	5.0	–	0.05	0.01	0.003
Water quality criteria for drinking water (mg L <sup>−1</sup> ) (WHO 2004)	0.05	0.07	–	5.0	–	2.0	0.01	0.003
Tributary (Mine adit water) (mg L <sup>−1</sup> )*	0.059	0.623	0.0048	0.0014	<0.004	<0.001	<0.01	–
Sediment of Cauvery river	389	28	–	93	–	11.2	4.3	1.3
Sediment of Tapti river	212	200	–	217	–	326	25	–
Sediment of tributary (Mine adit sediment)*	3561–3564	1939–1977	103.5–137.5	454–488	127.9–134.7	3.9–5.2	21.2–31.85	–
Sediment of Roro river*	322–330	55.5–57.5	69.4–139.5	553–558	23.8–28.5	16.4–21.3	35.3–40.7	–

All values are in mg kg<sup>−1</sup> unless it is not specified

\* Present study

substitution easily takes place in these Mg-rich minerals resulting in increase in concentration of Ni in mine waste (Bloise et al. 2010; Kumar and Maiti 2013). The mean pseudo-total Ni concentration of  $1225 \text{ mg kg}^{-1}$  was found in the top profile of CMW and increased with increase in depth may be because of the increase in silt and clay percentage (McGrath and Loveland 1992). High concentrations of Ni were found in the different layers of CAS1 and CAS2 with minimum concentration of  $108 \text{ mg kg}^{-1}$  in third profile of CAS2 may be because of the non-influence of Ni contamination in the deeper profile of distantly situated agricultural field. The CF in top profile of CMW, CAS1, and CAS2 was found above 24, which represents that the soil is very strongly contaminated with Ni. With increase in depth, the CF values for Ni decreased. Similarly, Igeo was ranged between 0.6 and 4.4 which represents that all the soils are heavily contaminated with Ni except last profile of CAS2.

#### *Zinc (Zn), manganese (Mn), and cobalt (Co)*

All the profiles of CMW were found low in Zn content resulting in improper and stunted growth of plants. The mean pseudo-total metal concentrations of Zn in three different profiles of 0–15 cm, 15–30 cm, and 30–45 cm were  $32 \text{ mg kg}^{-1}$ ,  $30 \text{ mg kg}^{-1}$ , and  $28 \text{ mg kg}^{-1}$  in CMW;  $47 \text{ mg kg}^{-1}$ ,  $42 \text{ mg kg}^{-1}$ , and  $30 \text{ mg kg}^{-1}$  in CAS1; and  $43 \text{ mg kg}^{-1}$ ,  $21 \text{ mg kg}^{-1}$ , and  $18 \text{ mg kg}^{-1}$  in CAS2, respectively. Das et al. (2013) had reported low concentrations of Zn ( $10\text{--}24 \text{ mg kg}^{-1}$ ) in the overburden dump of chromite. It was found that in most of the cases metal concentrations decreased with depth may be because of the lesser organic matter content in the lower profiles (Alloway 2013). However, CASs had little higher concentration of Zn as compared to CMW may be because of the addition of manure and P-fertilizer (Tang et al. 2014). The typical background concentration of Zn in soil ranged between 10 and  $100 \text{ mg kg}^{-1}$ , whereas the global average background concentration in soil is  $55 \text{ mg kg}^{-1}$  (Alloway 2013). However, these concentration values vary widely between soils.

The Mn and Co concentrations were found below the critical toxicity limit (Mn:  $1500\text{--}3000 \text{ mg kg}^{-1}$  and Co:  $25\text{--}50 \text{ mg kg}^{-1}$ ; Alloway 2013) in all the CMW and CASs samples. The Co, Mn, and Zn are the essential elements required by the plant for their proper growth and development. Because of the similar chemical properties, both Co and Mn remain closely related with each other in the soil. The ratio of Co:Mn was found 0.11 which was found close to the reported values of ultramafic soil (Levinson 1974). Significant differences ( $p < 0.05$ ) were found for the pseudo-total metal content in different sampling sites for the same profile. However, Co is of least concern in the environment when it is present in low concentration. The

pseudo-total concentration of Co under different depths was found ranged between  $7.4\text{--}11.1 \text{ mg kg}^{-1}$ ,  $6.3\text{--}9.5 \text{ mg kg}^{-1}$  and  $3.9\text{--}7.2 \text{ mg kg}^{-1}$  in the CMW, CAS1, and CAS2, respectively. Similarly, pseudo-total concentration for Mn ranged between  $373\text{--}444 \text{ mg kg}^{-1}$ ,  $303\text{--}400 \text{ mg kg}^{-1}$  and  $212\text{--}371 \text{ mg kg}^{-1}$  for different profiles of CMW, CAS1, and CAS2, respectively. Ho et al. (2013) had reported Mn concentration of  $683\text{--}832 \text{ mg kg}^{-1}$  in the abandoned site of serpentine mine. Percentage values of pseudo-total Co and Mn concentrations were about 17, 14, 13, 13 %, and 82, 87, 75, 63 % in the topsoil of CMW, CAS1, CAS2, and CS of its total content (data not shown), respectively.

The CF of Co and Mn was found decreasing with increase in depth and found none to moderate, whereas for Zn it was found below 1 representing no contamination. Similarly, Igeo of Mn, Co, and Zn for CMW, CAS1, and CAS2 was found below 0 to slightly above 1, which represents that the soil is unpolluted to moderately polluted.

#### *Copper (Cu), lead (Pb), and cadmium (Cd)*

The pseudo-total metal content of Cu and Pb was found low and below the critical soil total concentration in all the mine waste and soil samples. The background concentration of Cu typically depends on geology and varies between 2 and  $50 \text{ mg kg}^{-1}$  and normally  $60 \text{ mg kg}^{-1}$  exist in the earth's crust (Alloway 2013). Significant differences ( $p < 0.05$ ) were found for the pseudo-total metal content in different sampling sites for the same profile. Cu concentrations in top layer were ranged between  $30\text{--}36 \text{ mg kg}^{-1}$  and  $23\text{--}26 \text{ mg kg}^{-1}$  and  $12\text{--}24 \text{ mg kg}^{-1}$  in the CMW, CAS1, and CAS2, respectively. Similarly, Pb concentrations in top layer were ranged between  $5\text{--}9 \text{ mg kg}^{-1}$  and  $5\text{--}10 \text{ mg kg}^{-1}$  and  $2\text{--}07 \text{ mg kg}^{-1}$  in the CMW, CAS1, and CAS2, respectively. Percentage values of pseudo-total Cu and Pb concentration were about 28, 34, 35 %, and 10, 09, 13 % in the top profile of CMW, CAS1, and CAS2 of its total content (data not shown), respectively.

Cadmium is naturally occurring non-essential element present in divalent form and normally available in the range of  $0.1\text{--}1.0 \text{ mg kg}^{-1}$  in the soil with maximum up to  $3 \text{ mg kg}^{-1}$  (Alloway 2013; Gomez-Puentes et al. 2014). The Cd concentration was found low and ranged between 0.1 and  $1.1 \text{ mg kg}^{-1}$  in all the topsoil samples. However, Cd concentrations in top layer of CMW and CASs were found slightly higher than the normal soil. The pseudo-total metal concentrations of Cd were ranged between  $0.3\text{--}1.1 \text{ mg kg}^{-1}$ ,  $0.3\text{--}0.8 \text{ mg kg}^{-1}$  and  $0.2\text{--}0.7 \text{ mg kg}^{-1}$  in the three different profiles of 0–15 cm, 15–30 cm, and 30–45 cm of soil samples, respectively. The Cd and Pb concentrations were found slightly high in CASs soils than CMW may be because of addition of P-fertilizer (Alloway

2013; Tang et al. 2014; Guo and He 2013). Majority of Cd remains bound to organic matter in soils with pH < 6.5, whereas Fe-oxides become most important adsorptive constituent at pH > 6.5 (Buekers et al. 2008).

The CF and Igeo of Cu were ranged between 1–4 and –0.5 to 1.4, respectively, which suggests its non to moderate contamination. The CF and Igeo for Pb were found <0.5 and suggests no contamination. With increase in depth, CF of Cd increased and ranged between 3.2 and 4.5 suggesting its strong contamination, whereas Igeo was ranged between –1 and –1.6 suggesting its moderate contamination.

### Heavy metal concentrations in sediment and water samples

Concentration of heavy metals in the sediment samples and its corresponding concentration in water samples are presented in Table 5. High concentration above toxicity limits found for Cr and Ni with maximum concentration of 3561 mg Cr kg<sup>-1</sup> and 1957 mg Ni kg<sup>-1</sup> was found in the sediment sample of mine adit (from where underground mining was done). The concentrations of Cr (>0.05 mg L<sup>-1</sup>) and Ni (>0.02 mg L<sup>-1</sup>) in the mine adit water samples were also found high and above the critical water toxicity limit which shows the slow but continuous release of these potentially toxic metals in the environment. However, Cr concentration was found low (<0.05 mg L<sup>-1</sup>) for rest of the water samples collected from different areas. Concentration of Ni was found high (>0.02 mg L<sup>-1</sup>) in almost all the water samples suggesting its continuous contamination may be because of its higher solubility and mobility in water and sediment, respectively (Kumar and Maiti 2013). Tributaries flowing from the hill carrying huge volume of mine waste passing through the agricultural fields along with high concentration of different metals mix the Roro river and it further delivers in the major river of Jharkhand, Subernrekha. The concentrations of Cr and Ni were found high in the sediments of the pond which is being used by the farmers for local irrigation purpose. Use of such lands which are contaminated and deposited with mine waste sediments may result in accumulation of toxic metals in the crops and naturally growing local plants, and its regular consumption may transfer potentially toxic metals in human and livestock (Machender et al. 2013).

### Hierarchical cluster analysis

#### Source identification and metal grouping cluster analysis

The results obtained from cluster analysis (CA) revealed that Cr, Ni, and Mn were closely related to each other (Fig. 7a). The hierarchical cluster analysis using Ward's method produced three clusters; the first cluster contains

Co, Pb, Cu, and Cd, whereas the second cluster contains Mn and Zn and the third cluster contains only Cr and Ni. Cr is most distantly linked with the first and second group of clusters of metals and closely linked with Ni, revealing that the Cr has a single source of origin which is highly associated with Ni. Since, Cr and Ni are the transitional elements, these metals are closely related with each other (Das et al. 2013).

#### Spatial similarity and site grouping cluster analysis

Similarly, spatial CA was applied to group the different sampling sites CMW, CAS1, CAS2, and CS each with three different profiles of 0–15, 15–30, and 30–45 cm with the similar features/characteristics. Hierarchical CA was performed in all the sampling sites and it rendered a dendrogram (Fig. 7b). Dendrogram presented three clusters. Cluster 1 consists of non-metal influenced control soil and low contaminated agricultural soils of deeper profile: CS (0–15 cm), CS (15–30 cm), CS (30–45 cm), CAS2 (15–30 cm), and CAS (30–45 cm). Cluster 2 contains (CMW1, 0–15 cm; CMW, 15–30 cm; and CMW, 30–45 cm) highly Cr- and Ni-contaminated CMW sites. The third cluster contains the contaminated agricultural soils (CAS1, 0–15 cm; CAS1, 15–30 cm; CAS1, 30–45 cm; and CAS2, 15–30 cm) which are moderate to highly contaminated because of the influence of CMW and has very high and strong CF and Igeo values. The result showed that, because of the greater distance of CAS2 from CMW, thin layer was only deposited on the top profile of CMW resulting in moderate to high contamination. PCA has revealed that PC1 has contributed 57.8 % of total variance and mainly comprised of Cr and Ni with high loading values (Fig. 8). The first PC seemed to be associated to the earth's crust and geological formation of the area. The PC2 contributed to Mn and Zn and elucidated 22.6 % of total variance. This factor can be attributed to the previous mining activities of the area. PC3 contributed 12.5 % variance and includes other metals like Cd, Co, Cu, and Pb which may be because of the use of fertilizers in the agricultural fields. Complementary results of PCA and CA had also revealed that the Cr and Ni cluster together, whereas Mn and Zn are closely related and linked together. PCA suggested that the primary sources were anthropogenic, namely mining and extensive use of manures (Guo and He 2013).

### Conclusions

The present study revealed that the abandoned chromite-asbestos mine waste is acting as perennial source of contamination for the nearby agriculture fields. High

**Table 5** Concentration of heavy metals in the sediment (S) samples (mg kg<sup>-1</sup>) and its corresponding concentration in water (W) samples (mg L<sup>-1</sup>)

Sample no.	Cr		Ni		Zn		Mn		Co		Cu		Pb	
	S	W	S	W	S	W	S	W	S	W	S	W	S	W
S1	814.83 ± 1.53c (813.5–816.5)	<0.003	226.50 ± 2.78d (223.5–229)	<b>0.109</b>	134.83 ± 7.32a (127–141.5)	0.0020	577.67 ± 1.61a (576.5–579.5)	0.0032	40.75 ± 12.8c (28.5–54.15)	<0.004	63.23 ± 1.21a (62.3–64.6)	<0.001	25.30 ± 2.76b (22.45–27.9)	<0.01
S2	99 ± 3.28e (96.0–102.5)	<0.003	30.65 ± 1.79e (28–32)	<b>0.053</b>	83.67 ± 10.42d (74.5–95)	0.0038	226.50 ± 20.29d (207–247.5)	0.0006	21.50 ± 3.21de (19.5–25.2)	<0.004	17.31 ± 0.26bc (17.1–17.6)	<0.001	23.6 ± 1.41bc (22.5–25.2)	<0.01
S3	193.33 ± 1.04e (192.5–194.5)	<0.003	35.50 ± 3.12e (33–39)	<0.009	117.50 ± 23.5b (94.5–141.5)	0.0025	513.17 ± 22.01b (491.5–535.5)	0.0006	20.23 ± 1.55e (18.7–21.8)	<0.004	15.37 ± 1.06c (14.4–16.5)	<0.001	26.15 ± 0.74b (25.5–25.5)	<0.01
S4	326.67 ± 3.82d (322.2–330.0)	<0.003	56.53 ± 1.00 (55.5–57.5)	<b>0.021</b>	103.77 ± 35.0c (69.4–139.5)	0.0012	556.33 ± 2.89a (553–558)	0.0002	26.95 ± 2.68d (23.85–28.5)	<0.004	19.48 ± 2.66b (16.4–21.3)	<0.001	37.72 ± 2.79a (35.25–40.7)	<0.01
S5	867.67 ± 0.29c (867.5–868.0)	<0.003	614.60 ± 10.70c (602.5–622.8)	<b>0.065</b>	63.08 ± 3.07e (60.45–66.45)	0.0017	139.00 ± 6.26e (132.5–145)	0.0002	53.42 ± 3.55b (50.25–57.25)	<0.004	2.27 ± 0.21e (2.1–2.5)	<0.001	17.80 ± 4.85d (13–22.7)	<0.01
S6	3561.7 ± 1.89a (3561–3564)	<b>0.059</b>	1957.9 ± 34.0a (1939–1977)	<b>0.623</b>	121.83 ± 17.1b (103.5–137.5)	0.0048	469.33 ± 17.24c (454–488)	0.0014	131.17 ± 3.41a (127.9–134.7)	<0.004	4.63 ± 0.67d (3.9–5.2)	<0.001	27.18 ± 5.45b (21.2–31.85)	<0.01
S7	2095.6 ± 4.3b (2092–2100)	<0.003	1033.33 ± 3.79b (1029–1036)	<b>0.092</b>	96.50 ± 27.55c (68–123)	<0.0005	543.33 ± 63.62a (473.5–598)	0.006	43.12 ± 2.33bc (41.55–45.8)	<0.004	12.40 ± 9.38c (1.85–19.8)	<0.001	20.68 ± 8.25c (12.35–28.8)	<0.01
S8*	–	<0.003	–	<0.009	–	0.0025	–	0.006	–	<0.004	–	<0.001	–	<0.01
S9*	–	<0.003	–	<0.009	–	0.0015	–	0.006	–	<0.004	–	<0.001	–	<0.01
Detection limit	<0.003		<0.009		<0.0005		<0.0001		<0.004		<0.001		<0.01	

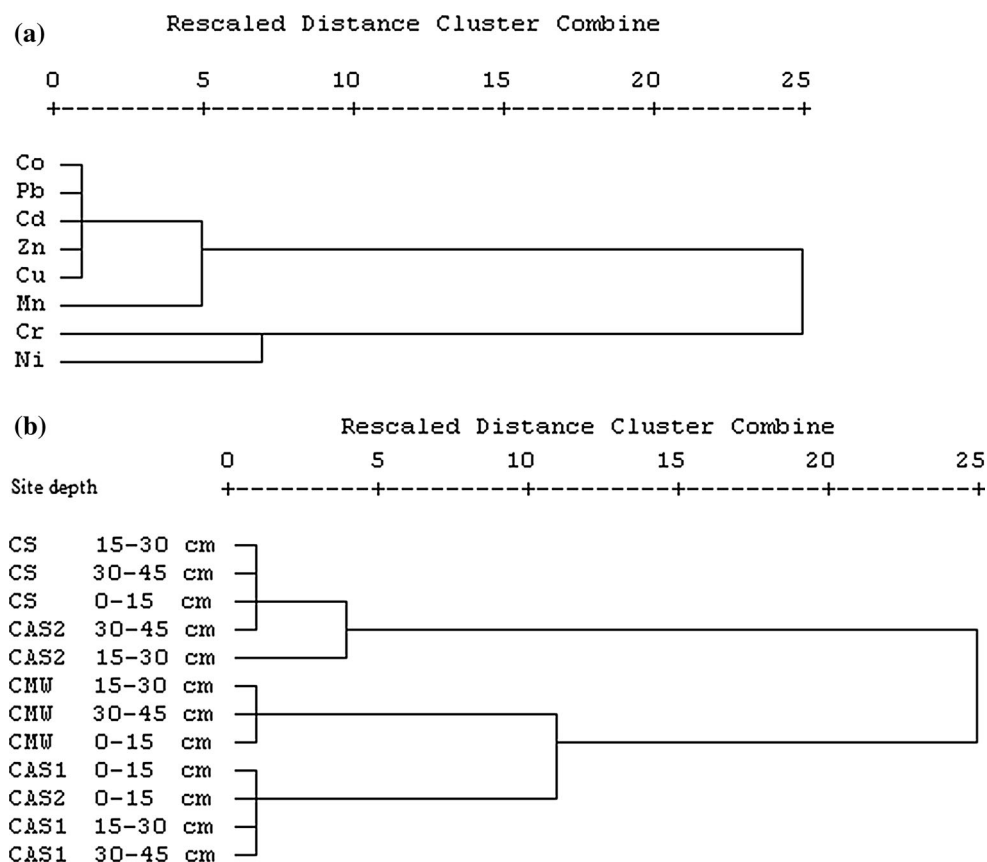
Different alphabetical letters in the same column represent significant difference at  $p < 0.05$  according to Duncan's multiple range test

Detection limits Cr: < 0.003; Ni: < 0.009; Zn: < 0.0005; Mn: < 0.0001; Co: < 0.004; Cu: < 0.001; Pb: < 0.01 mg kg<sup>-1</sup>

\* Only water samples were collected; Mean ± SD (Min–Max)

Bold values indicate concentrations of Cr and Ni above critical drinking water total concentration (IS 10500)

**Fig. 7** Hierarchical dendrogram showing **a** clustering of different metals, and **b** clustering of soil sampling sites with depth (0–15 cm, 15–30 cm, and 30–45 cm) using Ward's method



concentrations of Cr and Ni above soil toxicity limit were found in the contaminated agricultural soils (Fig. 8). The contamination factor and geoaccumulation index of the mine waste were found very high and strong for Cr and Ni, while for the other metals, it was found none to moderate. High concentrations of metal in all the

three profiles (0–45 cm) showed thick deposition of sediment in the nearby agricultural fields. Water flowing from the mine adit was found with significant concentration of Cr and Ni above critical drinking water total concentration. Cr concentration above toxicity limit was found in the sediment and water sample of tributary flowing from the hill. Metal grouping and site grouping cluster analysis have also revealed that Cr and Ni are closely linked with each other and mine waste is the major source of Cr and Ni contamination for the agricultural soils. Complementary results of FA and CA had further confirmed the association of Cr and Ni. Use of such lands which are contaminated and deposited with mine waste sediments may result in accumulation of toxic metals in the staple crops and naturally growing plants and its regular consumption may transfer potentially toxic metals in human and livestock. Though, practice of limited crops with low Cr and Ni accumulation and transfer ability is recommended, phytostabilization of waste is also essential by using organic manures and perennial aromatic grasses.

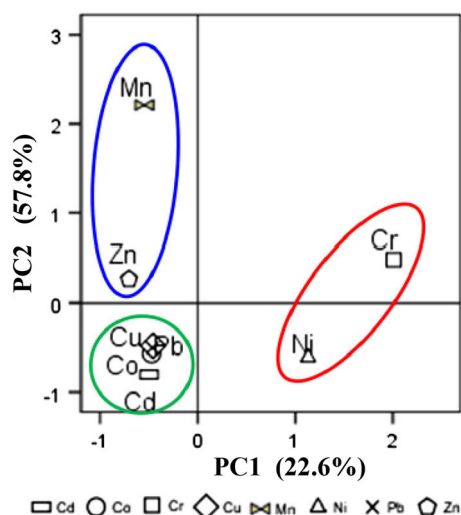


**Fig. 8** Principle component analysis for the heavy metals of soil samples

**Acknowledgments** The authors would like to thank Indian School of Mines, Dhanbad, India for providing the research facility and full scholarship to the main author. The authors are grateful to the scientific assistants Sarkar T and Ghosh SP for analyzing the samples.

Authors would also like to appreciate Sinku N for providing the assistance during the sampling and field work in FAAS.

**Conflict of interest** The authors declare that they have no conflict of interest.

## References

- Adriano D (2001) Trace elements in terrestrial environments: Biogeochemistry, bioavailability and risks of metals. Springer, New York
- Alloway BJ (1990) Heavy metals in soils. Wiley, New York
- Alloway BJ (2013) Heavy metals in soils: trace metals and metalloids in soils and their bioavailability. Environ Pollut 22, Springer, Dordrecht doi:10.1007/978-94-007-4470-7\_12
- APHA (2012) Standards for examination of water and wastewater, 22nd edn. American Public Health Association, Washington, DC
- Apollaro C, Marini L, Critelli T, Barca D, Bloise A, Rosa RD, Liberi F, Miriello D (2011) Investigation of rock-to-water release and fate of major, minor, and trace elements in the metabasalt–serpentine shallow aquifer of Mt. Reventino (CZ, Italy) by reaction path modelling Carmine. App Geochem 26:1722–1740
- Awasthi SK (2000) Prevention of food adulteration Act no 37 of 1954, Central and state rules as amended for 1999. Ashoka Law House, New Delhi
- Benhaddya ML, Hadjel M (2014) Spatial distribution and contamination assessment of heavy metals in surface soils of Hassi Messaoud, Algeria. Environ Earth Sci 71:1473–1486. doi:10.1007/s12665-013-2552-3
- Bloise A, Fornero E, Belluso E, Barrese E, Rinaudo C (2008) Synthesis and characterization of tremolite asbestos fibres. Eur J Miner 20:10271033
- Bloise A, Belluso E, Fornero E, Rinaudo C, Barrese E, Capella S (2010) Influence of synthesis condition on growth of Nidoped chrysotile. Microporous Mesoporous Mater 132:239245
- Buekers J, Amery F, Maes A, Smolders E (2008) Long term reactions of Ni, Zn and Cd with iron oxyhydroxides depend on crystallinity and structure and on metal concentrations. European J Soil Sci 59:706–715
- Cicchella D, Giaccio L, Lima A, Albanese S, Cosenza A, Civitillo D, Vivo BD (2014) Assessment of the topsoil heavy metals pollution in the Sarno River basin, south Italy. Environ Earth Sci 71:5129–5143. doi:10.1007/s12665-013-2916-8
- Das M, Maiti SK (2008) Comparison between availability of heavy metals in dry and wetland tailing of an abandoned copper tailing pond. Environ Monit Assess 137:343–350. doi:10.1007/s10661-007-9769-0
- Das S, Ram SS, Sahu HK, Rao DS, Chakraborty A, Sudarshan M, Thatoi HN (2013) A study on soil physico-chemical, microbial and metal content in Sukinda chromite mine of Odisha, India. Environ Earth Sci 69:2487–2497
- Fernandez-Caliani JC, Barba-Brioso C, Gonzalez I, Galan E (2009) Heavy metal pollution in soils around the abandoned mine sites of the Iberian pyrite belt (Southwest Spain). Water Air Soil Pollut 200:211–226. doi:10.1007/s11270-008-9905-7
- Gee GW, Bauder JW (1986) Particle-size analysis. In: Klute A (ed), Methods of soil analysis, Part 1 (2nd edn.), ASA and SSSA, Madison, WI pp 383–411 Agron. Monogr. 9
- Gomez-Puentes FJ, Reyes-Lopez JA, Lopez DL, Carreon-Diazconti C, Belmonte-Jimenez S (2014) Geochemical processes controlling the groundwater transport of contaminants released by a dump in an arid region of Mexico. Environ Earth Sci 71:609–621. doi:10.1007/s12665-013-2456-2
- GSI (2010) Geological Survey of India. Eastern Region Government of India Ministry of Mines. Base document on ferrous minerals (CGPB committee-i) Chromite Ore
- Guo CR, He X (2013) Spatial variations and ecological risk assessment of heavy metals in surface sediments on the upper reaches of Hun River, Northeast. Environ Earth Sci 70:1083–1090. doi:10.1007/s12665-012-2196-8
- Hakanson L (1980) An ecological risk index for aquatic pollution control of sediment ecological approach. Water Res 14:975–1000
- Ho CP, Hseu ZY, Chen NC, Tsai CC (2013) Evaluating heavy metal concentration of plants on a serpentine site for phytoremediation applications. Environ Earth Sci 70:191–199. doi:10.1007/s12665-012-2115-z
- Huang L, Deng C, Huang N, Huang X (2013) Multivariate statistical approach to identify heavy metal sources in agricultural soil around an abandoned Pb–Zn mine in Guangxi Zhuang Autonomous Region, China. Environ Earth Sci 68:1331–1348. doi:10.1007/s12665-012-1831-8
- IS 10500 (2012) Indian Standard, drinking water-specification, 2nd Revision, ICS 13.060.20, Bureau of Indian Standards, New Delhi
- Jackson ML (1973) Soil chemical analysis. Prentice Hall Pvt. Ltd., New Delhi
- Khorasanipour M, Aftabi A (2011) Environmental geochemistry of toxic heavy metals in soils around Sarcheshmeh porphyry copper mine smelter plant, Rafsanjan, Kerman, Iran. Environ Earth Sci 62:449–465. doi:10.1007/s12665-010-0539-x
- Kumar A, Maiti SK (2013) Availability of chromium, nickel and other associated heavy metals of ultramafic and serpentine soil/rock and in plants. Int J Emer Technol Adv Eng 3(2):256–273
- Kumar A, Maiti SK (2014) Translocation and Bioaccumulation of Metals in *Oryza sativa* and *Zea mays* growing in chromite-asbestos contaminated agricultural fields, Jharkhand, India. Bull Environ Contam Toxicol 93:434–441
- Levinson AA (1974) Introduction to exploration geochemistry. Applied Publishing, Calgary
- Li Y, Zhao H, Zhao X, Zhang T, Li Y, Cui J (2011) Effects of grazing and livestock exclusion on soil physical and chemical properties in desertified sandy grassland, Inner Mongolia, northern China. Environ Earth Sci 63:771–783. doi:10.1007/s12665-010-0748-3
- Lin C, He M, Liu X, Guo W, Liu S (2013) Distribution and contamination assessment of toxic trace elements in sediment of the Daliao River System, China. Environ Earth Sci 70:3163–3173. doi:10.1007/s12665-013-2382-3
- Machender G, Dhakate R, Rao GT, Loukya G, Reddy MN (2013) Assessment of trace element contamination in soils around Chinnaeru River Basin, Nalgonda District, India. Environ Earth Sci 70:1021–1037. doi:10.1007/s12665-012-2192-z
- Maiti SK (2013) Ecorestoration of the coalmine degraded lands. Springer, New York. doi:10.1007/978-81-322-0851-8
- Mathivanan K, Rajaram R (2014) Anthropogenic influences on toxic metals in water and sediment samples collected from industrially polluted Cuddalore coast, Southeast coast of India. Environ Earth Sci 72:997–1010. doi:10.1007/s12665-013-3017-4
- McGrath SP, Loveland PJ (1992) Soil geochemical Atlas of England and Wales. Blackie Academic & Professional, Glasgow
- Mileusnic M, Mapani BS, Kamona AF, Ruzicic S, Mapaure I, Chimwamurombe PM (2014) Assessment of agricultural soil contamination by potentially toxic metals dispersed from improperly disposed tailings, Kombat mine, Namibia. J Geochem Explor. doi:10.1016/j.gexplo.2014.01.009
- Moghaddas NH, Namaghi HH, Ghorbani H, Dahrzma B (2013) The effects of agricultural practice and land-use on the distribution and origin of some potentially toxic metals in the soils of Golestan province, Iran. Environ Earth Sci 68:487–497. doi:10.1007/s12665-012-1753-5

- Mukhopadhyay S, Maiti SK, Mastro RE (2013) Use of Reclaimed Mine Soil Index (RMSI) for screening of tree species for reclamation of coal mine degraded land. *Ecol Eng* 57:133–142. doi:[10.1016/j.ecoleng.2013.04.017](https://doi.org/10.1016/j.ecoleng.2013.04.017)
- Muller G (1969) Index of geoaccumulation in sediments of the Rhine River. *Geol J* 2:109–118
- Mushtaq N, Khan KS (2010) Heavy metals contamination of soils in response to waste water irrigation in awalpindi region. *Pak J Agrl Sci* 47(3):215–224
- Olsen SR, Sommers LE (1982) Phosphorus. In: Page et al. AL (eds) *Methods of soil analysis, part 2*, 2nd ed. ASA and SSSA, Madison, WI pp 403–430
- OSHA (2006) Occupational safety and health administration: health effects of hexavalent chromium. US department of labor, (800) 321. [www.osha.gov](http://www.osha.gov)
- Pugnalonia A, Giantomassi F, Lucarini G, Capell S, Bloise A, Primio RD, Belluso E (2013) Cytotoxicity induced by exposure to natural and synthetic tremolite asbestos: an in vitro pilot study. *Acta Histochem* 115:100–112
- Raju VK, Somashekar RK, Prakash KL (2012) Heavy metal status in river Cauvery, Karnataka. *Environ Monit Assess* 184:361–373. doi:[10.1007/s10661-011-1973-2](https://doi.org/10.1007/s10661-011-1973-2)
- Reeves RD, Baker AJM, Romero R (2007) The ultramafic flora of the Santa Elena peninsula, Costa Rica: a biogeochemical reconnaissance. *J Geochem Explor* 93:153–159. doi:[10.1016/j.gexplo.2007.04.002](https://doi.org/10.1016/j.gexplo.2007.04.002)
- Sharma SK, Subramanian V (2010) Source and distribution of trace metals and nutrients in Narmada and Tapi river basins, India. *Environ Earth Sci* 61:1337–1352
- Silva JD, Srinivasalu S, Roy PD, Jonathan MP (2014) Environmental conditions inferred from multi-element concentrations in sediments off Cauvery delta, Southeast India. *Environ Earth Sci* 71:2043–2058. doi:[10.1007/s12665-013-2606-6](https://doi.org/10.1007/s12665-013-2606-6)
- Sobek AA, Schuller WA, Freeman JR, Smith RM (1978) Field and laboratory methods applicable to Overburden and Minesoils, USEPA Rep. 600/2-78-054, US Gov. Print. Office, Washington, DC
- Subbiah BV, Asija GL (1956) A rapid procedure for the determination of available nitrogen in soil. *Curr Sci* 25:259–260
- Tang W, Ao L, Zhang H, Shan B (2014) Accumulation and risk of heavy metals in relation to agricultural intensification in the river sediments of agricultural regions. *Environ Earth Sci* 71:3945–3951. doi:[10.1007/s12665-013-2779-z](https://doi.org/10.1007/s12665-013-2779-z)
- USEPA 3050B (1996) Acid digestion of sediments, sludge and soils. Revision 2 3050B pp 1–12. <http://www.epa.gov/osw/hazard/testmethods/sw846/pdfs/3050b.pdf>
- Varol M, Gokot B, Bekleyen A (2013) Dissolved heavy metals in the Tigris River (Turkey): spatial and temporal variations. *Environ Sci Pollut Res Int* 20(9):6096–6108. doi:[10.1007/s11356-013-1627-8](https://doi.org/10.1007/s11356-013-1627-8)
- Walkley A, Black IA (1934) An examination of the Degtjareff method for determining soil organic matter and a proposed modification of the chromic acid titration method. *Soil Sci* 37:29–38. <http://libra.msra.cn/Publication/43474065>
- Wang L, Wang Y, Zhang W, Xu C, An Z (2014) Multivariate statistical techniques for evaluating and identifying the environmental significance of heavy metal contamination in sediments of the Yangtze River, China. *Environ Earth Sci* 71:1183–1193. doi:[10.1007/s12665-013-2522-9](https://doi.org/10.1007/s12665-013-2522-9)
- Whalley C, Hursthouse A, Rowlat S, Iqbal-Zahid P, Vaughan H, Durant R (1999) Chromium speciation in natural waters draining contaminated land, Glasgow, UK. *Water Air Soil Pollut* 112:389–405
- WHO (2004) Guidelines for drinking-water quality, 3rd ed., vol 1. Recommendations. World Health Organization, Geneva
- Zhang D, Zhang X, Tian L, Ye F, Huang X, Zeng Y, Fan M (2013) Seasonal and spatial dynamics of trace elements in water and sediment from Pearl River Estuary, South China. *Environ Earth Sci* 68:1053–1063. doi:[10.1007/s12665-012-1807-8](https://doi.org/10.1007/s12665-012-1807-8)
- Zhao K, Zhang W, Zhou L, Liu X, Xu J, Huang P (2009) Modeling transfer of heavy metals in soil–rice system and their risk assessment in paddy fields. *Environ Earth Sci* 59:519–527. doi:[10.1007/s12665-009-0049-x](https://doi.org/10.1007/s12665-009-0049-x)